10th ANKARA INTERNATIONAL AEROSPACE CONFERENCE **AIAC-2019-047**
18-20 September 2019 - METU, Ankara TURKEY

THE INFLUENCE OF THE AXIAL GAP LENGHT BETWEEN ROTOR AND STATOR ON TONAL NOISE OF TRANSONIC AXIAL COMPRESSOR

Bora Yazgan[1]
Istanbul Technical University
Istanbul, Turkey

Erkan Ayder[2]
Istanbul Technical University
Istanbul, Turkey

ABSTRACT

This article describes the computational aeroacoustics calculations to investigate the effect of the axial gap length between the rotor and the stator of a transonic axial compressor stage on the tonal (discrete) noise generation. NASA Stage 37 test case was selected as the investigated transonic axial compressor stage. Computational fluid dynamics model of the transonic compressor stage with three different axial gap length between the rotor and stator were formed. Unsteady Reynolds Averaged Navier Stokes Equations (URANS) were solved for capturing nearfield acoustics. For the farfield acoustic propagation the unsteady rotor and stator blade pressure values from the URANS simulations were imported to Ffowcs Williams and Hawkings (FW-H) acoustic solver. The CFD results shows that the potential field between the rotor and stator and the interaction of the rotor wake and stator strongly decayed as the axial gap length increases. This resulted in an observable reduction in the tonal noise generation at blade passing frequency (BPF) and its higher harmonics.

INTRODUCTION

In multi-stage turbomachinery applications, an interaction takes place between the rotating blades (rotor) and stationary vanes (stator). This interaction may take place in different mechanisms including potential field of the blades and the rotor wake-stator vane interactions. Both causes strong tonal noise generation. Potential effect stems from the presence of adjacent blade rows. In axial compressors presence of the stator vanes in the downstream of the rotor blades forms fluctuations in the static pressure field in neighbor of the rotor and stator. Potential effect can become severe when the axial gap length between the rotor and the stator decreases. It is stated that 85% to 95% of the unsteady loading on the blades can be generated by the potential field [Sadek, 2015]. Moreover, a numerical analysis of a subsonic rotor stage showed that stator potential field is the second major tonal noise source on the rotor blades [Laborderie and Soulat and Moreau, 2014].

As stated the other source of the rotor-stator interaction noise is the rotor wake-stator vane interaction in axial compressors. The rotor wake is defined as deficit in axial velocity and increase in tangential velocity, which impinges the stator vane with a higher incident angle. This impingement takes place periodically at the blade passing frequency (BPF) and results in

[1] Graduate Student in Mechanical Engineering, Email: yazganbo@itu.edu.tr
[2] Professor in Mechanical Engineering, Email: aydere@itu.edu.tr

pressure fluctuations having same frequency as BPF and its higher harmonics on the entire surface of the stator vanes. The tonal noise generation mechanism of the wake was attributed to upwash velocity [Laborderie and Soulat and Moreau, 2014]. Upwash velocity constitutes the normal velocity component to the stator vane. As seen on the velocity triangles in Figure 1 relative velocity of wake $W_{2,wake}$ is lower than the bulk flow relative velocity W_2. That is why the absolute velocity of the wake $C_{2,wake}$ impinges the stator blade with a higher incidence than the absolute velocity of the bulk flow C_2 does. Thus, a velocity component that is normal to the stator vanes occurs as called upwash velocity $C_{2,upwash}$. This unsteady velocity component of $C_{2,upwash}$ impinges stator leading edge at the BPF and generates pressure fluctuations at the stator surface by changing angle of attack. It was stated that the rotor wake-stator vane interaction rather than the stator potential field dominantly generates unsteady forces on the blades [Gallus, 1997]. It was also claimed that viscous wake interactions were the predominant tonal noise source for the blade rows used in fans and compressors [Walker, 1971].

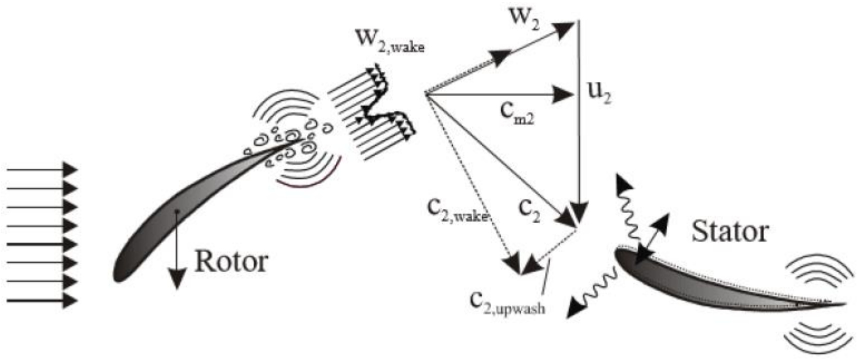

Figure 1: Upwash Velocity

METHOD

The axial gap length has strong effect on the interaction tonal noise of the compressor stage. The effect of potential field decreases strongly as the axial gap between the rotor and stator row increases. Amplitude of the potential effect-generated unsteady pressure fluctuation vanishes quickly with the increasing axial gap but the wake interactions shows a slightly decreasing trend [Gallus, 1997]. It was stated that noise reduction up to 6 or 8 dB is possible by incerasing the axial gap [Hünecke, 1997]. Moreover, in another study doubling axial gap between the rotor and stator resulted in approximately 4 dB noise reduction [Benzakein, 1974].

Because of the strong effect of axial gap between the rotor-stator on the noise generation, the rotor-stator interaction tonal noise was investigated with three different transonic axial compressor stage, each having different axial gap between rotor and stator. Flow field aerodynamics of each case, especially the stator potential field on rotor and the rotor wake-stator interaction, was investigated in order to understand how the noise sources and noise propagation are affected by the flow. Case 1 that is the original geometry of the NASA Stage 37 has the axial gap 8 mm between rotor blades and stator vanes at 50% span. Case 2 and case 3 have the axial gap of 16 mm and 32 mm respectively as seen in Figure 2.

Computational Fluid Dynamics Model

In Star CCM+ computational fluid dynamics calculations were conducted for each case by solving URANS equations. Although aeroacoustic computations requires LES based turbulence models in order to capture acoustic waves properly, URANS method was resorted since URANS models can be prefferred when flow features are certainly tonal like blade passing frequency. Moreover, significant amount computational effort was saved by resorting URANS. K-ω SST turbulence model was utilized for URANS equations. It is reported that URANS method is quite appropriate for the blade bassing frequency tones prediction of turbomachinery applications and generally gives satisfying results compare to experiments [Holewa and Lesnik and Ashcroft and Guerin, 2017]. In another CFD based study, it is stated that URANS simulations are efficient and accurate methods to obtain turbomachinery tonal noise soruces. [Moreau, 2019].

Computational fluid dynamics model domain of each case and boundary conditions are shown in Figure 3. Original NASA Stage 37 has 46 stator vanes. However, in this study, number of the stator vanes were equilized to the rotor blades (36) in order to provide a pitch ratio of 1. This facilitates the modeling and saves the computational effort.

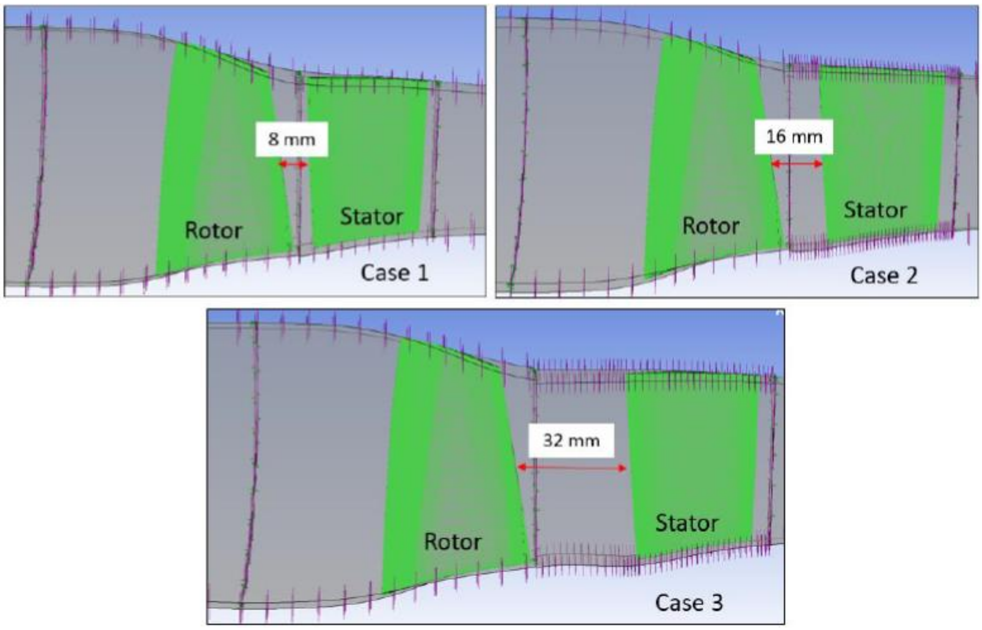

Figure 2: Different axial gap configurations of NASA stage 37 transonic axial compressor stage

The computational fluid dynamics model consist of extended stationary inlet, rotating rotor, stationary stator and extended outlet domains. Periodic boundary conditions were utilized one each side in order to represent full wheel. Rigid body motion method was applied to simulate the motion of the rotor blade. Unsteady implicit coupled solver was selected with the time step of 9.696×10^{-7} s which corresponds to 0.1° rotation of rotor blades in tangential direction. This means rotor blade completes one blade passing with 100 time steps. Other numerical modeling specifications and the boundary conditions are shown in Figure 4.

Meshing

Acoustic wavelength is the determinant factor for the meshing. Best practices for the second order numerics proposes at least 20 elements per wavelength to capture the acoustic waves. The acoustic wave with the upper frequency has the minimum wavelength. For the near-field acoustics, the upper frequency limit was determined as the fourth harmonics of the BPF. This means that the tonal noise up to the fourth harmonics of the BPF can be captured by this simulation setup, whilst the higher harmonics may undergo a numerical dissipation. Number of elements for case 1, case 2 and case 3 are 3,818,890, 3,840,279, 4,174,407 respectively.

Moreover, resolving the boundary layer on rotor and stator blade is another significant factor that should be considered for meshing. Since the compressor is operated under transonic conditions, a shock wave take places in front of the rotor blade and this interact with the boundary layer of the adjacent rotor blade which result in boundary layer separation. Hence, in order to capture this, y+ values must be below 5 for selected turbulence model k-ω SST.

Boundary Conditions

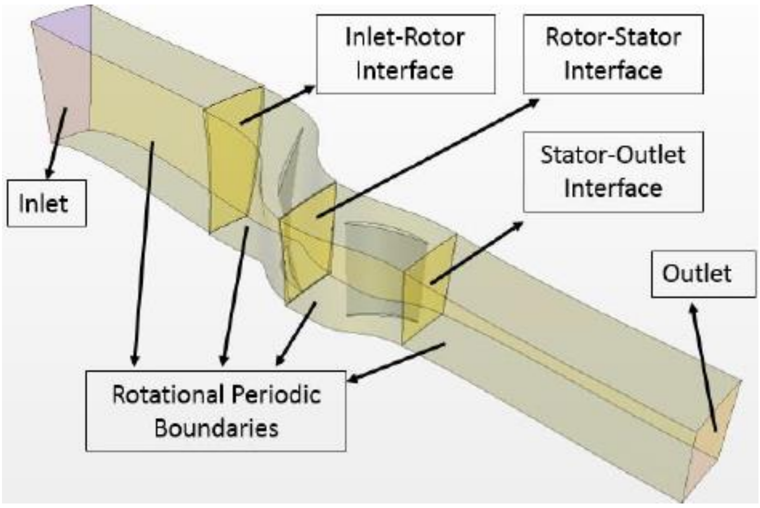

Figure 3: CFD domain and boundary conditions of compressor stage

URANS Simulation Numerical Model Details	
Solver	Unsteady Implicit Coupled Solver
Rotation Modeling	Rigid Body Motion
Material	Air Ideal Gas
Time Step Size	9.696×10^{-7} s
Rotational Speed	17188.7 rpm
Inlet Absolute Total Pressure	101325 Pa
Inlet Total Temperature	288.15 K
Outlet Absolute Static Pressure	145000 Pa
Turbulence Model	SST k-ω

Figure 4: Modeling specifications and boundary conditions

Near field noise

The near-field noise investigation is based on processing the pressure data obtained by CFD solution near the source region. A couple of pressure probes as seen in Figure 5 were located adjacent to the stator vane in order to calculate the noise level on these probes in terms of sound pressure level. Totally nine pressure probes were located at midspan in each case as they surrounds the stator vane. The noise spectrum at these probes were calculated by applying Fast Fourier Transform (FFT) on recorded unsteady pressure data.

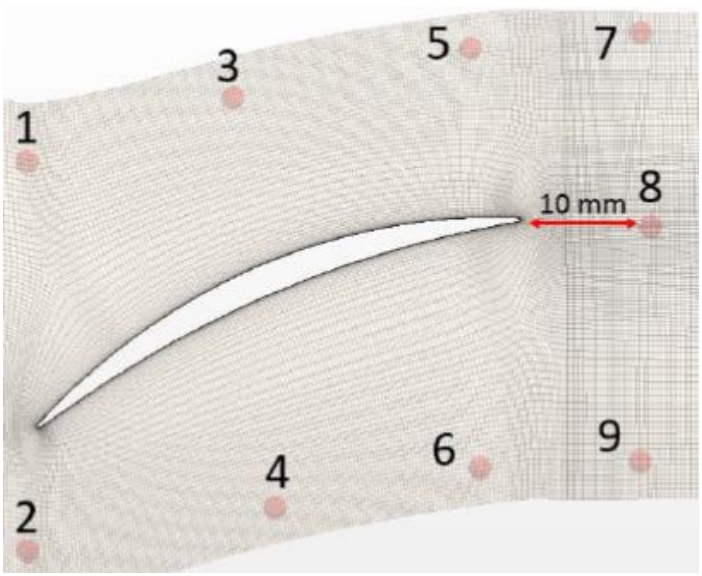

Figure 5: Near field pressure probes.

Far field noise

As a hybrid method URANS simulation and FW-H acoustic analogy was utilized to calculate the far-field noise of the compressor stage. In the first step URANS simulation was run to collect unsteady pressure data on the noise source locations which are rotor and stator blade surfaces. Then this data was imported as input for FW-H solver to calculate the noise at far field receivers. These receivers are located out of the CFD domain. The distance between the stator blade and the farthest receiver is 0.7 meter. The workflow of this method and the observer locations are shown in Figure 6 and Figure 7 respectively.

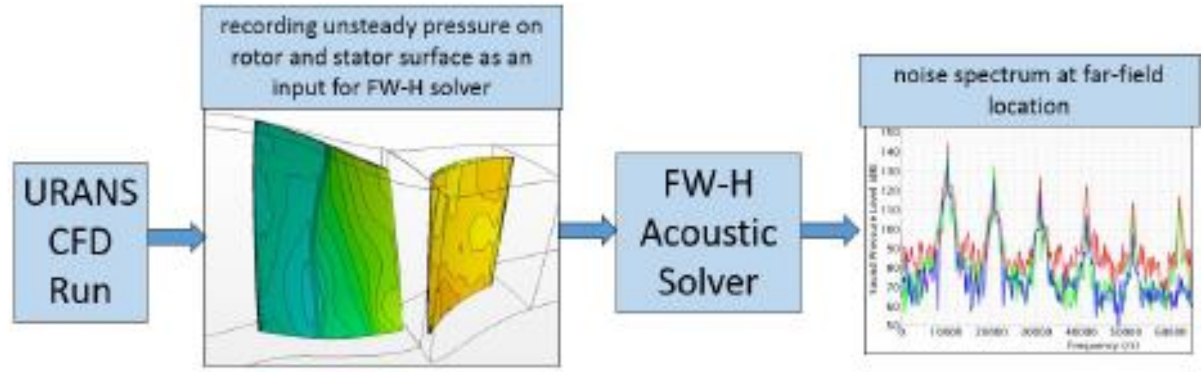

Figure 6: Far field noise calculation workflow.

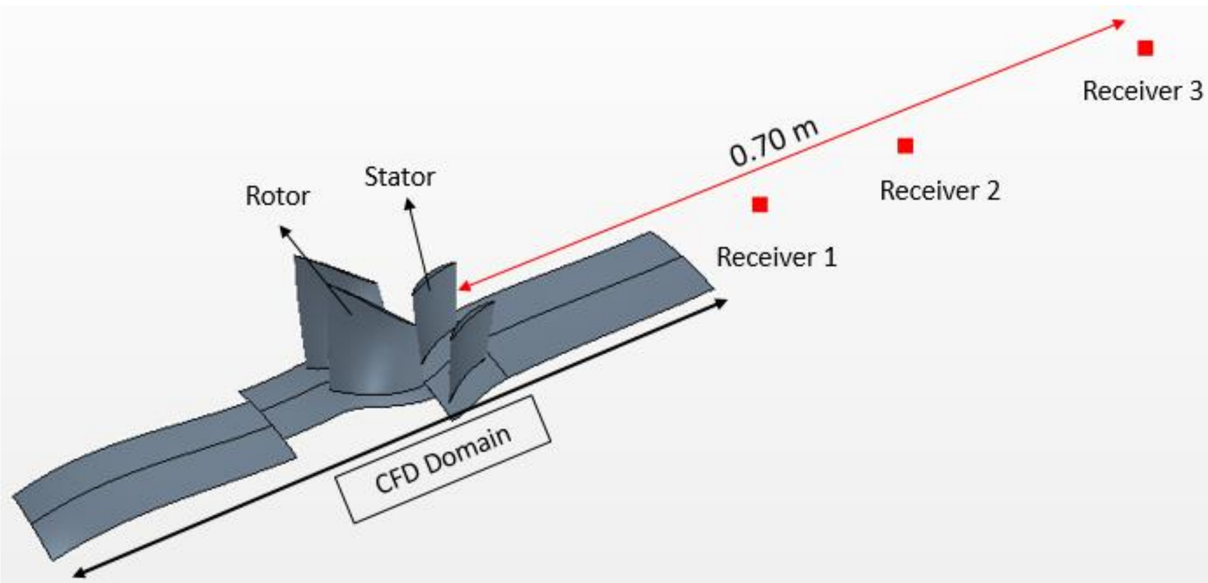

Figure 7: FW-H observer locations.

RESULTS

Near field noise

Regarding the near field noise investigation recorded pressure data and noise spectrum of probe 1 for each cases are shown in Figure 8 and Figure 9 respectively. The amplitude of the unsteady pressure is larger for the case 1 that has the shortest axial gap between rotor and stator. As the axial gap increases the amplitude of the pressure signal decreases. This proves that the interaction between the rotor and stator significantly increases with the smaller axial gap. The noise spectrum of probe 1 shows that the tonal noise and the broadband noise of the case 1 is dominant over the other cases.

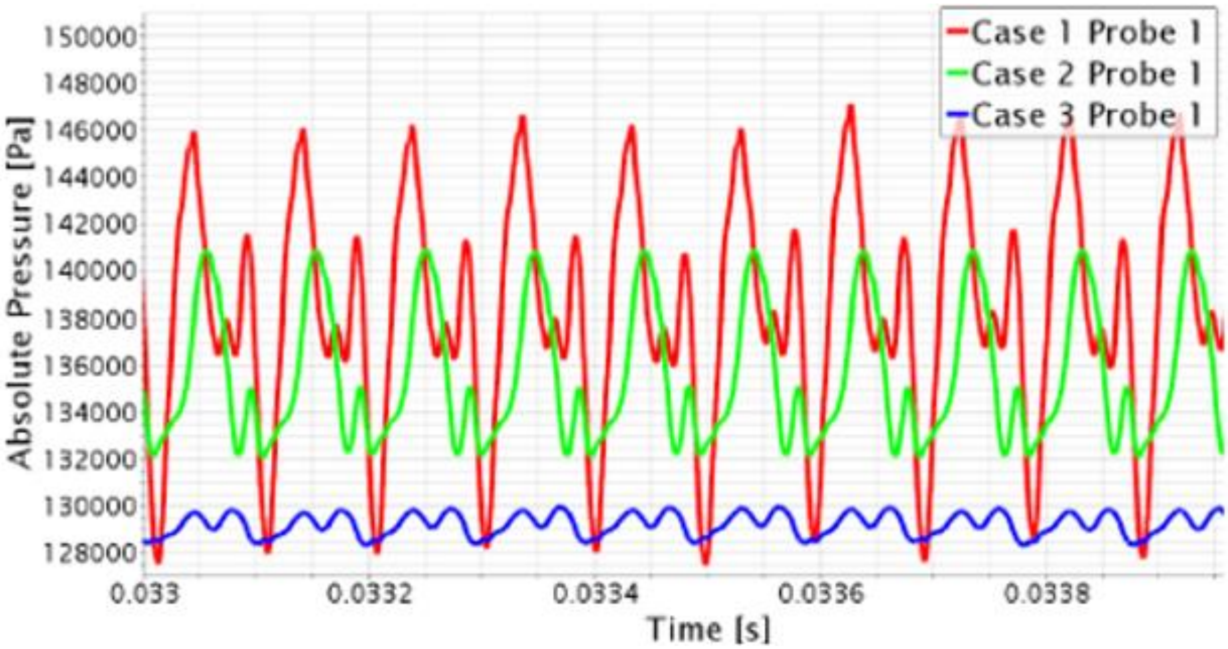

Figure 8: Recorded pressure data on near field probe 1.

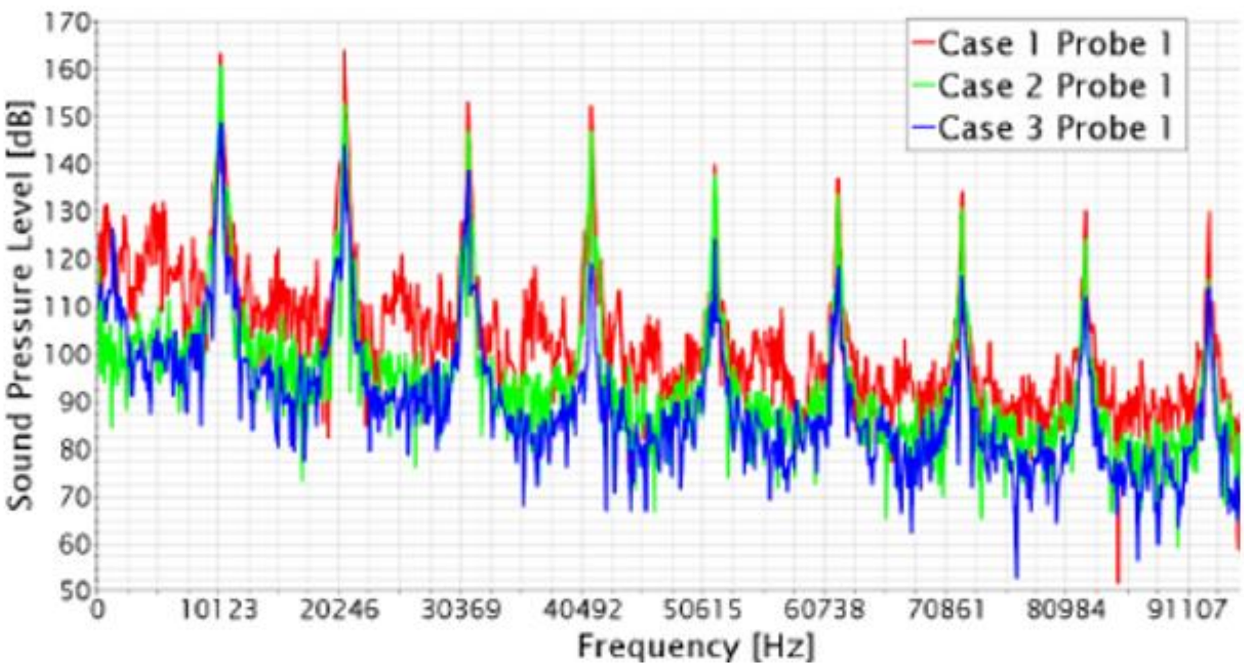

Figure 9: Noise spectrum (right) on near field probe 1.

As seen in Table 1, the tonal noise values at first three blade passing frequencies decrease as the axial gap between the rotor and stator increases. A noise reduction of 5-10 dB is observable for the first tone which is the most effective noise source. The noise suppression for second BPF is larger compared to first tone.

Probe	Case	1^{st} BPF	2^{nd} BPF	3^{rd} BPF
Probe 1	Case 1	163.3	163.8	153.0
	Case 2	160.6	152.8	146.6
	Case 3	148.7	144.0	138.5
Probe 2	Case 1	168.2	158.8	150.4
	Case 2	158.0	147.4	143.8
	Case 3	148.7	144.0	138.5
Probe 3	Case 1	170.3	151.6	150.2
	Case 2	161.3	146.0	136.4
	Case 3	157.3	145.8	140.8
Probe 4	Case 1	165.6	166.0	154.3
	Case 2	160.8	150.8	144.7
	Case 3	151.5	137.5	135.1
Probe 5	Case 1	161.7	161.0	143.4
	Case 2	156.8	155.8	145.3
	Case 3	153.6	142.5	110.3
Probe 6	Case 1	165.0	154.1	151.6
	Case 2	156.3	148.0	145.2
	Case 3	153.8	143.9	130.5
Probe 7	Case 1	171.4	164.3	152.7
	Case 2	166.0	161.2	139.4
	Case 3	163.3	150.1	135.0
Probe 8	Case 1	162.0	157.5	141.9
	Case 2	161.7	138.7	132.7
	Case 3	149.8	117.4	121.2
Probe 9	Case 1	159.6	160.2	144.2
	Case 2	156.5	148.9	133.7
	Case 3	152.0	142.2	125.4

Table 1: Noise values [dB] of first three tones at near-field pressure probes.

Figure 10 illustrates the results of the space time plot post processing feature on the midspan section of the stator pressure side. Space time plot represents the magnitude of the normalized unsteady pressure across a line from leading edge to trailing edge of a blade [Sadek, 2015]. The y axis consists of the sampling points on the line from leading edge to trailing edge while the x axis shows the time steps. In this case, x axis contains 500 time steps which coresspond totally 5 blade passing time. As seen, case 1, which has the minimum axial gap, has the highest unsteady pressure magnitude on stator surface. As the axial gap increases, the magnitude of the unsteady pressure on stator surface decreases. Moreover, it is observable that the unsteadiness on the stator blade reaches the highest value near the leading edge and gradually decreases in the streamwise direction to the trailing edge. In brief, space time plots on midspan section of pressure side of the stator blade shows that the unsteady pressure fluctuations increases as the axial gap decreases which causes the stator blade to be a stronger noise source.

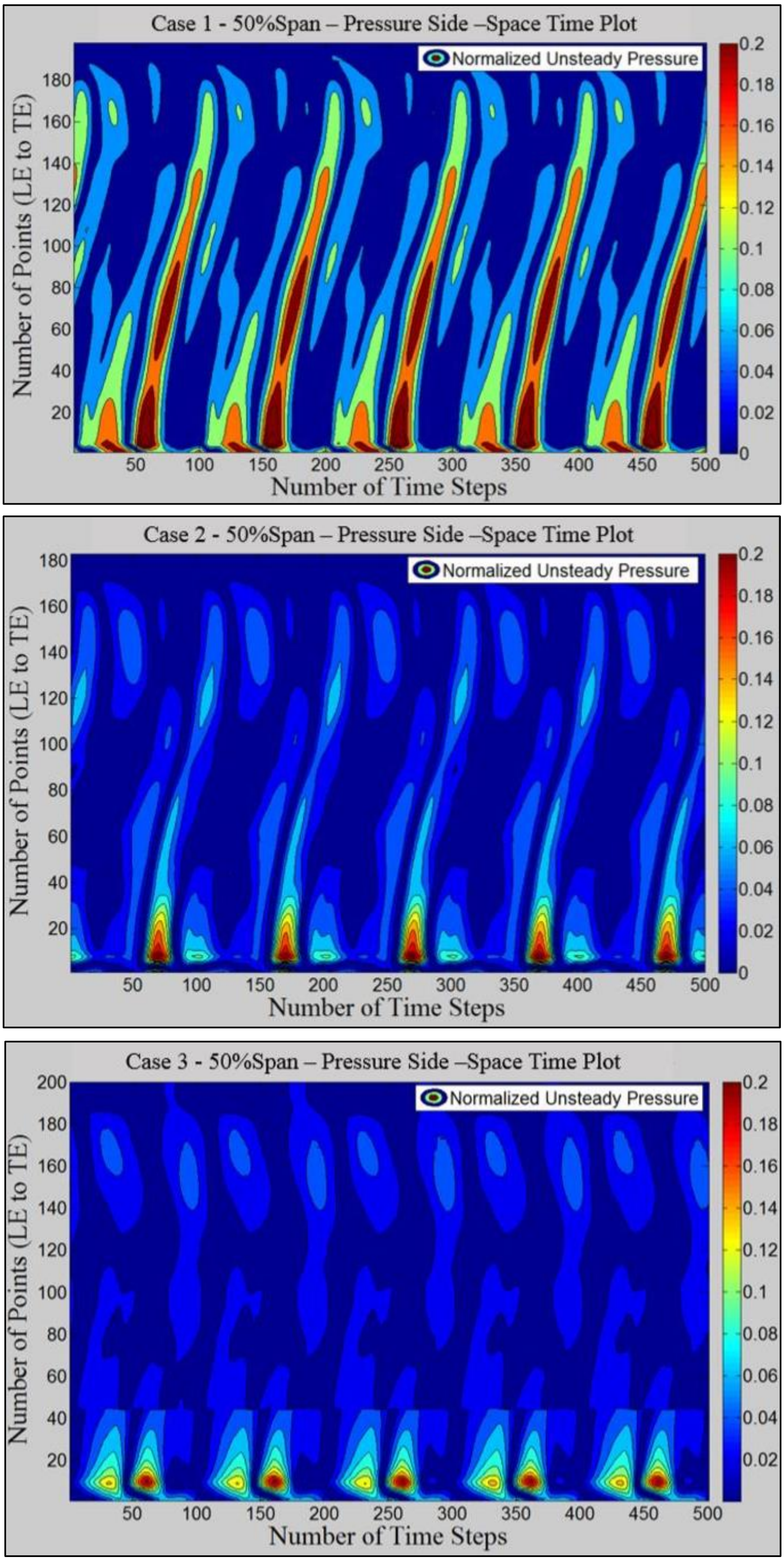

Figure 10: Space time plots on midspan of stator blade pressure side.

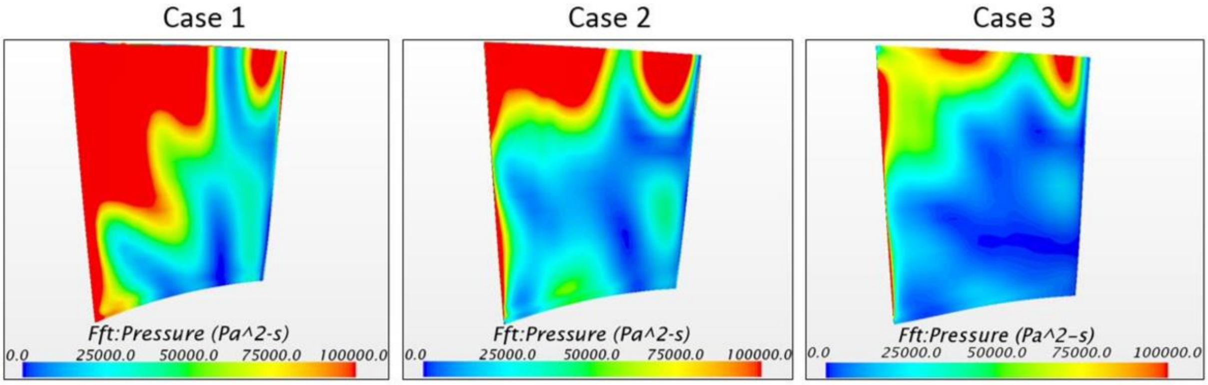

Figure 11: Power spectral density distribution on stator pressure surface at 1st BPF.

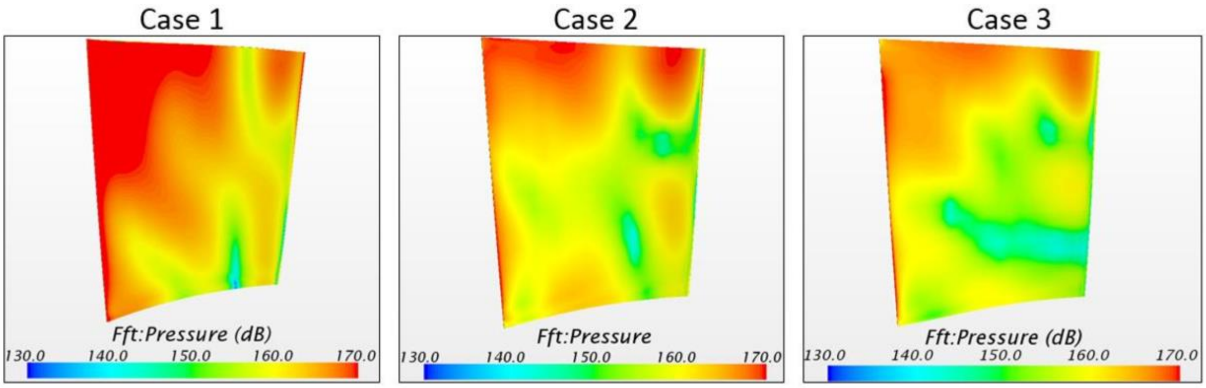

Figure 12: Sound pressure level [dB] distribution on stator pressure surface at 1st BPF.

Figure 11 and Figure 12 show the power spectral density (PSD) and sound pressure level (SPL) on stator pressure side at 1st BPF. Power spectral density is related to energy of pressure fluctuations. PSD and SPL were calculated by applying Fast Fourier Transform (FFT) on the acquired pressure signal on stator surface. As seen, as the axial gap increases the energy of pressure fluctuation and SPL values decrease. It is also observable that, the sound generation on stator surface is denser at leading edge and near shroud.

Far field noise

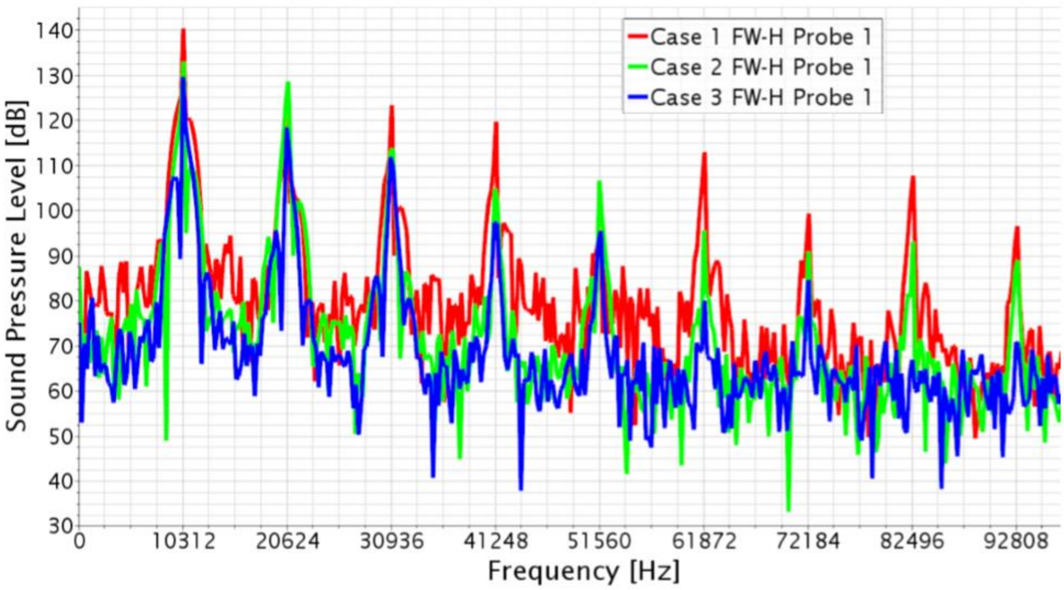

Figure 13: Noise spectrum on far field probe 1.

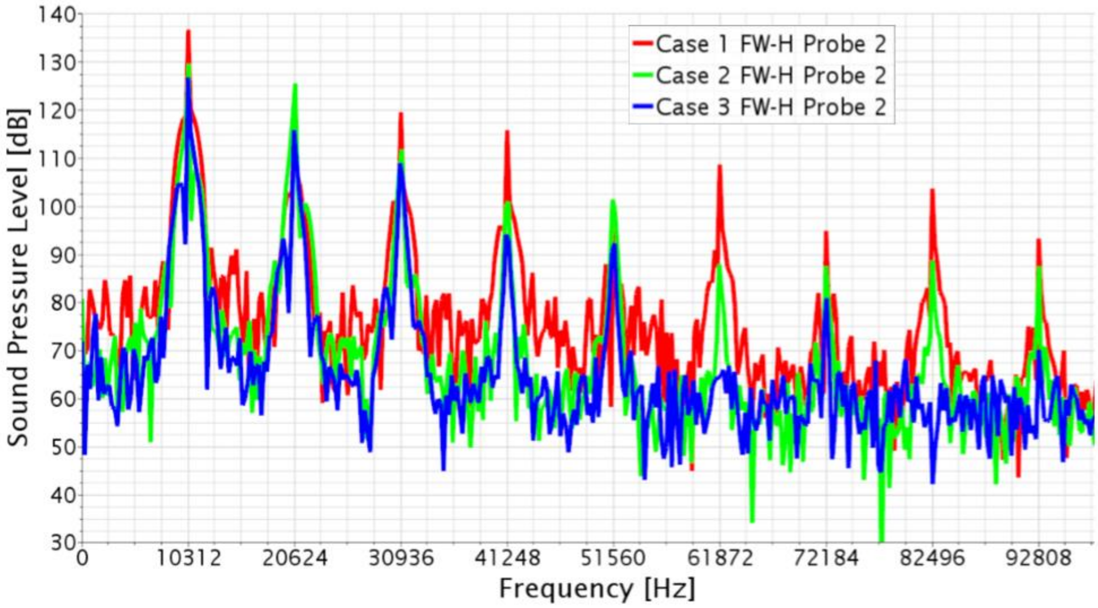

Figure 14: Noise spectrum on far field probe 2.

Figure 13 and Figure 14 illustrate the noise spectrum at far field receivers 1 and 2 respectively. According to results, apart from the 2nd BPF, increasing the axial gap is an effective way to decrease the tonal noise generation. Moreover, these figures verifies that the magnitude of the generated noise decay as the sound waves propogate further from the source. Although, turbulence noise sources were not included in FWH solution, the broadband noise generation is higher for case 1.

Noise values in terms of dB are listed for the first three blade passing frequency in Table 2.

FW-H Probe	Case	1st BPF	2nd BPF	3rd BPF
Probe 1	Case 1	140.3	125.5	123.3
	Case 2	132.9	128.6	114.5
	Case 3	129.6	118.3	111.8
Probe 2	Case 1	136.7	121.8	119.5
	Case 2	129.6	125.5	111.8
	Case 3	126.7	115.9	109.0
Probe 3	Case 1	132.8	117.6	115.6
	Case 2	125.9	121.9	109.0
	Case 3	114.6	109.7	100.1

Table 2: Noise values [dB] of first three tones at far-field pressure probes

Increasing axial gap length between the rotor and stator resulted in an efficiency loss as shown in Table 3. As seen, doubling the axial gap length yielded 1% isentropic efficiency loss.

Case	Isentropic Efficiency [%]
Case 1	82.04
Case 2	81.17
Case 3	80.19

Table 3: Isentropic efficiency of stage

CONCLUSIONS

Increasing the axial gap length between the rotor and stator is an effective way to reduce the tonal noise generation of the axial compressor stage since this method mitigate the potential effects between the rotor and stator and the rotor wake stator interactions. Significant noise reduction was observed for both near-field and far-field observers. However, increasing the axial gap resulted in an efficiency loss. Thus, efficieny loss is a restriction of increasing the gap length. It is a trade-off between the aerdoynamic loss and noise reduction.

URANS method is appropriate to capture the tonal noise at each blade passing frequency values.

References

Benzakein, M.J. (1974) *Research on Fan Noise Generation*, The Journal of the Acoustical Society of America

Gallus, H.E. (1997) *Experimental Investigation of Rotor-Stator Interaction in Axial-Flow Turbines and Compressors*. Institut für Strahlantriebe und Turboarbeitsmaschinen, RWTH Aachen

Holewa, A., Lesnik, S., Ashcroft, G., & Guerin, S.(2017). CFD-Based Investgation of Turbine Tonal Noise Induces by Steady Hot Streaks. *International Journal of Turbomachinery, Propulsion and Power, 2*(1), 3.

Hünecke, K.A. (1997) *Jet Engines: Fundamentals of Theory, Deisgn and Operation,* 1st Edition

Laborderie, J. & Soulat, L. & Moreau S., (2014). *Prediction of Noise Sources in Axial Compressor from URANS Simulation.* University of Sherbrooke.

Moreau, S. (2019). *Turbomachinery Noise Predictions: Present and Future.* Universite de Sherbrooke, QC, Canada

Sadek, J. (2015), *Effect of Axial Gap Distance on Transonic Compressor Performance.* Royal Institute of Technology. Stockholm.

Walker, G.J., (1971), *Effect of Wake-Wake Interactions on the Noise Generated by an Axial Flow Compressor.* Monash University. Melbourne.